

Abdenour Bouakache¹, Aichouche Belhadj-Aissa¹, Gregoire Mercier²

¹Image Processing and Radiation Laboratory,
University of Science and Technology Houari Boumediene,
BP. 32, El Alia, Bab Ezzouar,
16111, Algiers, Algeria.
abbouakache@lycos.com, h.belhadj@lycos.com

²Institut Telecom, Telecom Bretagne,
CNRS UMR 3192 Lab-STICC/CID,
Technopole Brest-Iroise CS 83818,
29238 Brest Cedex3, France.
Gregoire.Mercier@telecom-bretagne.eu

Satellite image fusion using Dezert-Smarandache theory

Published in:

Florentin Smarandache & Jean Dezert (Editors)

Advances and Applications of DSMT for Information Fusion
(Collected works), Vol. III

American Research Press (ARP), Rehoboth, 2009

ISBN-10: 1-59973-073-1

ISBN-13: 978-1-59973-073-8

Chapter XXII, pp. 549 - 564

Abstract: *Free and hybrid models of multisource satellite images fusion are developed using the plausible and paradoxical reasoning theory of Dezert-Smarandache. The aim of this work is to show the contribution of these fusion models for improving the thematic classification and the quantification of change. The maps obtained by the free model are composed by simple classes and compound classes. Nevertheless, they contain no significant thematic classes and require an important computing time. In the other hand, the hybrid model with a constraint introduced using a prior knowledge relatively of the study area, can have maps composed of more realistic classes in a reduced time. These models are implemented and tested on images acquired by SPOT HRV and Landsat ETM+ sensors.*

22.1 Introduction

Recently, the number of satellite sensors is growing. Information acquired by the various satellite sensors is very rich and complementary. The combination or the fusion of different types of information become very interesting. It must take into account the sources of information increasingly numerous and varied. Information fusion resulting from different sources remains an open and important problem. The difficulty of this process is due to both uncertain and conflicting information available.

In this context, several approaches and theories have been developed [2, 5, 13, 17]. The probabilistic approach which is the oldest and most widespread, it can represent well the uncertainty in the information but does not represent its imprecision [2]. Moreover, it reasons on only simple classes that represent different hypothesis. However, the Dempster-Shafer Theory (DST) can be an alternative to the probabilistic approach, it is often recommended and used by some authors [2, 3, 10–12] because it can also put up with the uncertain nature of information through a solid mathematical formalism and Dempster combination rule.

Nevertheless, this theory has certain weaknesses when the combined evidence sources become very conflicting (conflict close to the unit) and when the problem to be processed cannot be directly described within the frame of discernment of this theory due the paradoxical nature of information. Consequently a new theory which can be considered as a generalization of DST was elaborate, it is the plausible and paradoxical reasoning theory of Dezert-Smarandache (DSmT) [6, 7, 13, 14], it was applied in the field of remote sensing by [3, 4]. This theory can solve some delicate problems where DST is usually fails.

DSmT starts with the notion of free DSm model. This model is free because no other assumption is done on the hypotheses. When the free DSm model holds, the classic commutative and associative DSm rule of combination is performed. In this free model, the rule of combination takes into account both uncertain and paradoxical information. Thus, it generates a frame of discernment more general. But, if the cardinal of this frame increases the computing time increases and moreover some classes of the power set are not significant. Therefore, a integrity constraints are explicitly and formally introduced into the free DSm model in order to adapt it properly to fit as close as possible with the reality and permit to construct the hybrid model. There exist actually many possible hybrid models between the two extreme models (Shafer model and free model) for the frames depending on the real intrinsic nature of elements. The hybrid DSm rule works in any model and is involved in calculating the combined mass of any number of information sources, no matter how big is the conflict/paradoxism of sources, and on any frame (exhaustive or non-exhaustive, with elements which may be exclusive or non-exclusive or both) [13].

The aim of our work is the improvement of the thematic classification and the quantification of changes by a fusion process of optical satellite images using two models of DSmT (the free and the hybrid models). These images are covering a zone of study located at the east of Algiers.

The remainder of the paper is organized as follows. In the next section, we recall the mathematical basis of DSmT and its application to fusion process. Section 22.3 is devoted to the presentation and the implementation of the free model and the hybrid model of DSmT. In section 22.4, the two models of DSmT will be applied to the fusion of two multisource and multitemporal images. Finally, section 22.5 gathers our conclusions and the possible prospects to this work.

22.2 Dezert Smarandache theory basis

The DSmT of plausible, uncertain and paradoxical reasoning [6, 8, 9, 13, 15] is a generalization of the classical DST [5, 16] which allows to formally combine any types of sources of information (rational, uncertain or paradoxical). The DSmT is able to solve complex data/information fusion problems where the DST usually fails, especially when conflicts (paradoxes) between sources become large and when the refinement of the frame of discernment Θ is inaccessible because of the vague, relative and imprecise nature of Θ elements. The foundation of DSmT is based on the definition of the hyper-power set D^Θ (Dedekind's lattice) of a general frame of discernment Θ [8, 9]. The foundation of DSmT is based on the definition of the hyper-power set D^Θ [8, 9] which detailed in section 1.2.1 of the chapter 1, in the beginning of this book.

22.2.1 Mass functions

The determination of mass functions in DSmT represents a crucial step in a fusion process and remains a largely unsolved problem, which did not yet find a general answer. In image processing, Bloch [2] describes three different levels from where a mass function may be derived: at the highest level where information representation is used in a way similar to that in artificial intelligence and masses are assigned to propositions; at an intermediate level, masses are computed from attributes, and may involve simple geometrical models; at the pixel level, mass assignment is inspired from statistical pattern recognition. Recall that the difficulty increases when we are interested on the compound hypotheses and their mass functions. The most widely used approach is to assign to simple hypotheses masses that are computed from conditional probabilities. Then a transfer model is introduced to distribute the initial masses over all compound hypotheses (union and intersection of classes). This transfer operation is done through a coarsening (discounting) factor and/or a conditioning factor applying to the conditional probabilities (initial masses).

In this paper, the mass functions are estimated using a dissonant model of Appriou that was initially developed for only two classes [1] and we have generalized and extrapolated for more than two classes as follows [3]. In the following equations, x_s^b stands for the value of a pixel of the SPOT or Landsat image at spectral band b and

spatial location s .

$$\forall i = 1, \dots, k \quad m_i^b[x_s^b](\theta_i) = \frac{\alpha_i^b R^b P(x_s^b|\theta_i)}{1 + R^b P(x_s^b|\theta_i)} - \frac{|D^\Theta| - k - 2}{k} \varepsilon \quad (22.1)$$

$$\forall r = 1, \dots, k; r \neq i; k \neq 1 \quad m_i^b[x_s^b](\theta_r) = \frac{\frac{\alpha_i^b}{k-1}}{1 + R^b P(x_s^b|\theta_i)} - \frac{|D^\Theta| - k - 2}{k} \varepsilon$$

$$m_i^b[x_s^b](\theta_1 \cup \theta_2) = m_i^b[x_s^b](\theta_1 \cup \theta_3) = \dots = m_i^b[x_s^b](\theta_1 \cup \dots \cup \theta_{k-1}) = \varepsilon$$

$$m_i^b[x_s^b](\theta_1 \cap \theta_2) = m_i^b[x_s^b](\theta_1 \cap \theta_3) = \dots = m_i^b[x_s^b](\theta_1 \cap \dots \cap \theta_{k-1}) = \varepsilon$$

$$m_i^b[x_s^b](\Theta) = 1 - \alpha_i^b,$$

where k is the number of the considered classes, ε is a sensitivity factor that weighted the mass functions in order to have their sum over all the hypothesis equal to 1, $P(x_s^b|\theta_i)$ is the conditional probability, α_i^b is a coarsening factor, and R^b represents a normalization factor that is introduced in the axiomatic approach in order to respect the mass and plausibility definitions, and is given by:

$$R^b = \frac{1}{\max_{i=1, \dots, k} P(x_s^b|\theta_i)}.$$

To fuse paradoxical or rational sources of information (bodies of evidence), we have used in this paper the DSM classical rule and the DSM hybrid rule. These rules are detailed in the sections 1.2.4 and 1.2.5 of the chapter 1 in this book.

For a future work, we plan to test the PCR5 for the multi-source satellite image fusion. This rule redistributes every partial conflict only to propositions only which are truly involved in it and proportionally to their masses put in the conflict [15].

22.2.2 Decision Rule

After the combination of different sources, a decision is made according to a certain criteria. Several decision rules have been proposed:

1. maximum of plausibility which is advocated by some authors [2–4, 11, 12],
2. maximum of belief over the simple hypothesis which is the most used [11],
3. maximum of belief without overlapping of belief intervals which is very strict and called absolute decision rule [3, 11, 12],
4. maximum of pignistic probability [13, 17].

22.3 Implementation of the free and hybrid models

22.3.1 Implementation of the free model

The fusion process with the free model $\mathcal{M}^f(\Theta)$ is given in Fig. 22.1.

The fusion process is detailed by the following steps:

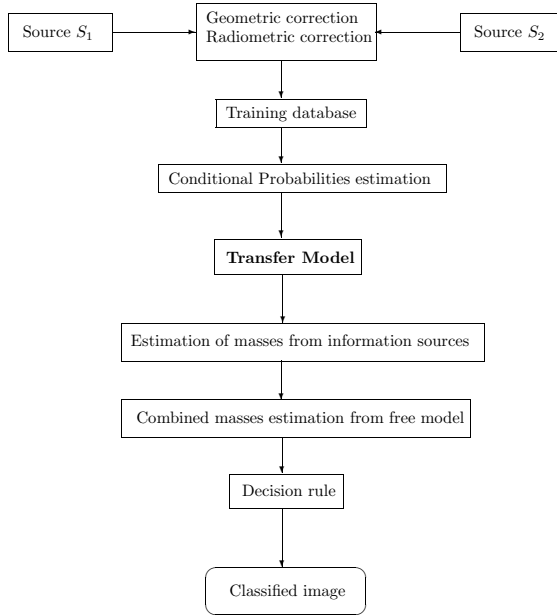


Figure 22.1: Multi-source fusion process using the free model.

1. A geometrical correction in the same reference frame using the interpolation by the polynomial model.
2. A radiometric corrections for both images.
3. According to an *a priori* knowledge, two data bases are constructed: a training base to be used in a supervised classification process, and a test base to be used during the assessment of the classification accuracy.
4. A Bayesian classification is performed using a maximum likelihood algorithm.
5. A confusion matrix is established between a Bayesian classification result and a test data base.
6. For each class, a coarsening factor is obtained from the confusion matrix and it can be seen as the accuracy of that class which is computed by dividing the total number of correct pixels in that class by each of the total number of pixels in that category as derived from the test data base.
7. The mass function is estimated using transfer model of Appriou, detailed in sec. 22.2.1.

8. The mass function is estimated one more time by using transfer model of Ap-
priou.
9. A combination rule of DS_mT between sources is applied to obtain the combined
mass S_1 given by:

$$S_1(A) \triangleq \sum_{\substack{X_1, X_2, \dots, X_k \in D^\Theta \\ X_1 \cap X_2 \cap \dots \cap X_k = A}} \prod_{i=1}^k m_i(X_i) \tag{22.2}$$

10. The combined mass S_1 is saved.
11. The belief and the plausibility functions are deduced from the combined mass
function.
12. The uncertainty for each pixel is calculated.
13. Finally, a multispectral classification is released according to a decision rule.

22.3.2 Implementation of the hybrid model

The fusion process with the hybrid model $\mathcal{M}(\Theta)$ is given in Fig. 22.2 and detailed by the following steps.

1. Introduction of the combined mass S_1 calculated in the free model $\mathcal{M}^f(\Theta)$.
2. Introduction of the constraints by forcing some elements of D^Θ to be empty.
3. Determination of the characteristic non-emptiness function $\phi(A)$ and the total
empty set $\emptyset \triangleq \{\emptyset_{\mathcal{M}}, \emptyset\}$.
4. Calculation of the sum based on the technique of absorption, transferred the
mass from each empty element to total or relative ignorance using the expres-
sion of S_2 (see section 1.2.5 in chapter 1) given by:

$$S_2(A) \triangleq \sum_{\substack{X_1, X_2, \dots, X_k \in \emptyset \\ [U=A] \vee [(U \in \emptyset) \wedge (A=I_t)]}} \prod_{i=1}^k m_i(X_i) \tag{22.3}$$

5. Calculation of the sum transferred the masses of relative empty sets to nonempty
sets using the following expression of S_3 (see section 1.2.5 in chapter 1):

$$S_3(A) \triangleq \sum_{\substack{X_1, X_2, \dots, X_k \in D^\Theta \\ X_1 \cup X_2 \cup \dots \cup X_k = A \\ X_1 \cap X_2 \cap \dots \cap X_k = \emptyset}} \prod_{i=1}^k m_i(X_i) \tag{22.4}$$

6. Calculation of the combined masses using the general rule of hybrid combination of DSm [7] defines as follows:

$$\forall A_i \in D^\Theta, \quad m_{\mathcal{M}(\Theta)}(A_i) = \phi(A_i) [m_{Mf(\Theta)}(A_i) + S_2(A_i) + S_3(A_i)].$$

7. The belief and the plausibility functions are deduced from the combined mass function.
8. The uncertainty for each pixel is calculated.
9. Finally, a multispectral classification is released according to a decision rule.

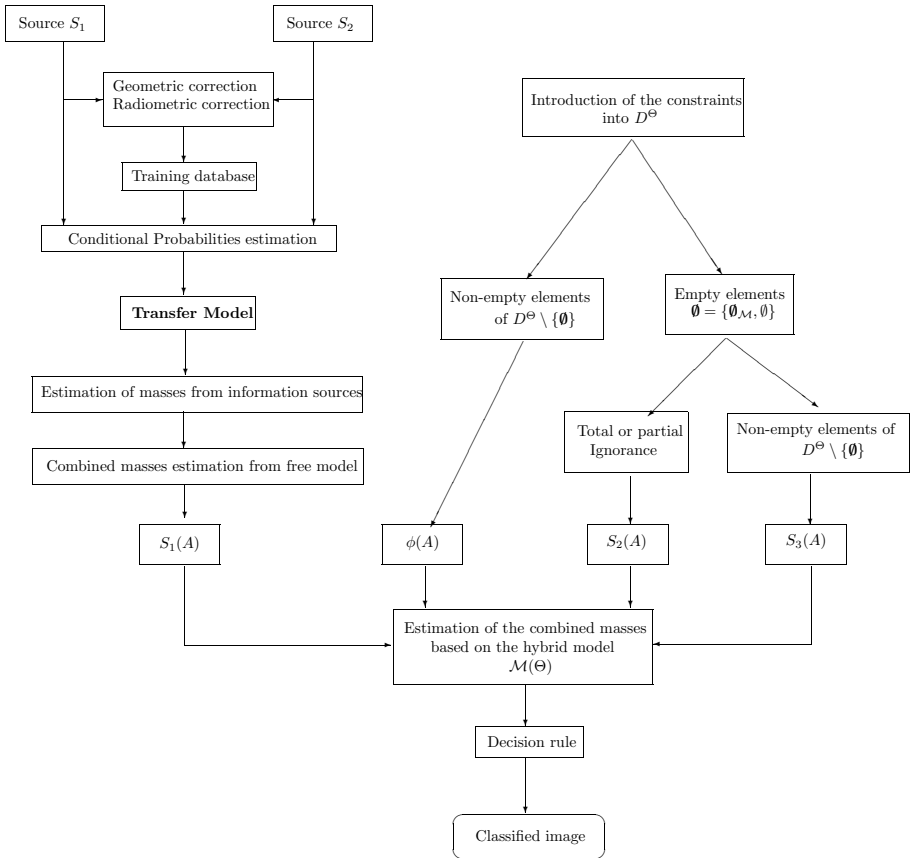


Figure 22.2: Multi-source fusion process using the hybrid model.

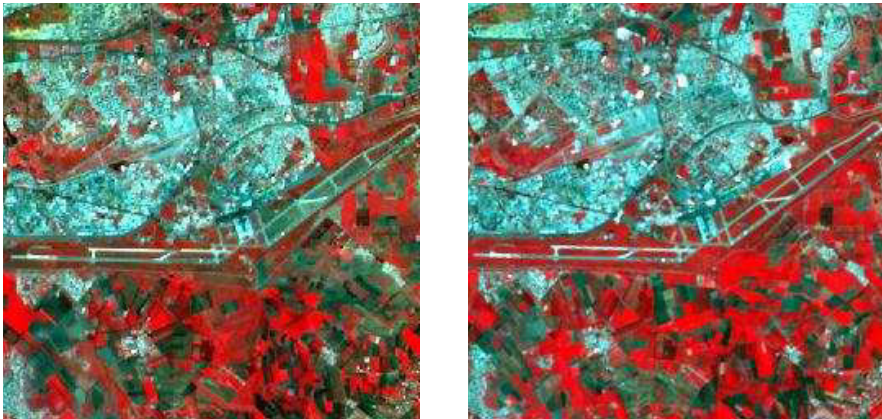
22.4 Application

22.4.1 Site of study and data used

The methodology proposed is tested on an area located approximately at 10km to the east of Algiers. This area is characterized by high urban concentration and a very dense road network in the north of the airport and an agricultural area with bare soil in the south of the airport.

For a multisource study of the site, we often used a data set acquired by different satellite sensors at the same date on the same study area and for a multitemporal study of the site, it is preferable to use a data set acquired by the same sensor on different times on the same scene. However, currently we do not have this ideal data set. Therefore, two multisource and multitemporal images were put at contribution in this study: a multispectral image acquired on April 1st, 1997 by the sensor HRV1 of SPOT-1 satellite, a multispectral image acquired on June 3rd, 2001 by the sensor ETM+ of Landsat-7 satellite. The joint exploitation of these images requires a step of geo-referencing through a method of geometric correction.

In our case, we applied the polynomial method through a second order polynomial. Then, we proceeded to the resampling of HRV image at a resolution of 30 m using the method of Nearest Neighbour. Thus, the RGB compositions of the two images corrected are shown in Fig. 22.3.



(a) SPOT HRV 1997

(b) Landsat ETM+ 2001

Figure 22.3: RGB composition of the Algiers scene, Algeria.

The methodology of fusion and classification adopted in this work is supervised based on a prior knowledge on the study site and the various themes which are there. Then, we extracted a training base and a test base for each image. These bases contain three thematic classes: Dense Urban (DU), Bare Soil (BS) and Vegetation (V) that have been identified and defined by an expert knowing well this area of study.

The validity of the choice of the three classes for the steps of training and evaluation is carried out and justified in [10]. Indeed, for the two images, we notice that the difference between the envelope of the three normal distributions associated with the three classes and the form of the real histogram is very negligible. This means that the two images are dominated by the three classes considered.

22.4.2 Fusion based on the free model

In a multitemporal study of a site, it is preferable to use a multitemporal data set acquired by the same satellite sensor on the same study area. However, we do not have this data set. Therefore, two multisource and multitemporal images were used in this study.

The improvement of the land cover maps obtained is based on the joint exploitation of the two essential characteristics of the sensors which provide the images. The first characteristic is the wealth of the spectral information of the image acquired by sensor ETM+ (six spectral bands) which allows a better identification and discrimination of the themes on the ground, and the second characteristic is the wealth of the spatial information of the image acquired by the sensor HRV (spatial resolution of 20 m) which allows a more detailed description of the objects.

The result of multisource classification and fusion obtained by the free model is given by Fig. 22.4.

The evaluation of this result will focus only on the invariant sites between the two dates of acquisition (1997 and 2001). The airport's runways are considered as invariant site and have not undergone any changes between the two dates of acquisition.

We note, from Fig. 22.4, that the multisource image obtained by the free model and more exactly the sites invariant of the airport's runways, constitute of the simple classes DU on which the two sensors of acquisition (ETM+ and HRV) give the same opinion with certainty, and of the compound classes (intersection of classes) like the classes $U \cap V$, $(BS \cup V) \cap U$ and $BS \cap V$, on which the two sensors give different opinions, *i.e.*, there is a confusion between the two sensors.

By taking a pixel located in the airport's runways, belonging to the class of intersection $U \cap V$ generated by the free model, we note that its spectral signature in image HRV corresponds to the signature of the class U, and that its signature in image ETM+ thus corresponds to the signature of the class V, the attribution of this

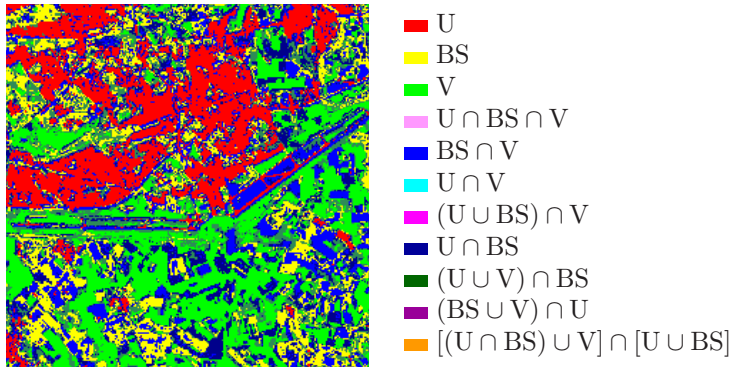


Figure 22.4: Result of multi-source fusion based on the free model. U: Urban area, V: Vegetation, BS: Bare soil.

pixel to the class $U \cap V$ is well justified (see Fig.22.5).

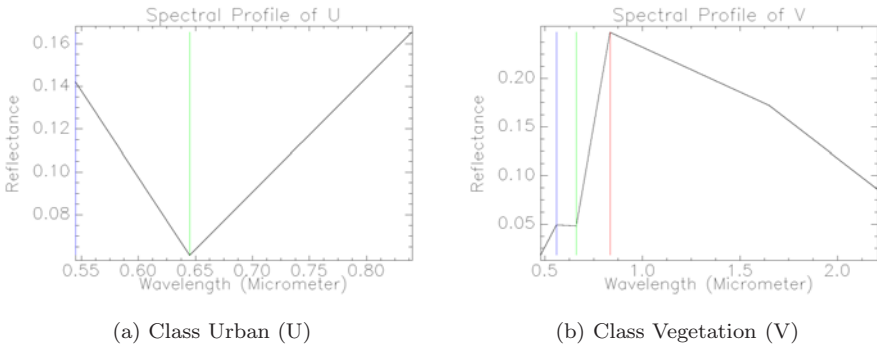


Figure 22.5: Spectral signatures of the classes Urban (HRV 1997) and Vegetation (ETM+ 2001) in the invariant site of airport’s runways by the free model.

The evaluation of the result in the case of multitemporal fusion will carry only on the sites varying between the two dates (1997 and 2001). We take as an example of variant sites, an agricultural zone located at the south of the airport.

We note that the multitemporal image obtained by the free model in more exactly the variant sites, constitute of simple classes representing the stable zones as the class V not having undergone any change, and of the compound classes representing the zones of changes during the time considered, as the class of intersection $BS \cap V$ which is an unstable zone.

By taking a pixel, located in the agricultural zone, belonging to the class $BS \cap V$ generated by our methodology, we notice that its spectral signature in image HRV corresponds to the signature of the class BS, and that its signature in image ETM+ corresponds to the signature of the class V (Fig. 22.6). Therefore, the attribution of this pixel which changed class BS towards V to the class $BS \cap V$ is well justified.

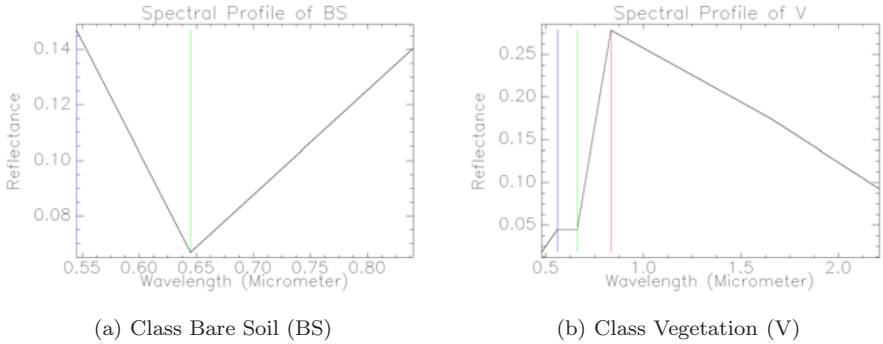


Figure 22.6: Spectral signatures of the classes Bare soil (HRV 1997) and Vegetation (ETM+ 2001) in the variant site of the agricultural zone by the free model.

The result of the binary changes detection between 1997 and 2001 by multisource and multitemporal classification and fusion using the free model is given in Fig. 22.7. The simple classes represent the no change (in black), on the other hand the compound classes represent the change (in white).

From a qualitative evaluation of this image, we see that there are a great dynamics in the study area between the two dates considered, an evolution of the thematic classes “bare soil” and “vegetation” in the south of the airport which is due one side, to the clearing of the land agricultural and another side to the farm of the bare areas and a dense urbanization in the north of the airport, in particular in the area of El Hamiz.



Figure 22.7: Binary changes image between 1997 and 2001 obtained by the free model.

22.4.3 Fusion based on the hybrid model

From a prior knowledge on the study area, we take as constraint, the proposition: $U \cap V$. Therefore, the set of the focal elements of D^Θ is reduced to the following set:

$$\{U, BS, V, U \cup BS, U \cup V, BS \cup V, U \cup BS \cup V, U \cap BS, BS \cap V, (U \cup V) \cap BS, (U \cap BS) \cup V, (BS \cap V) \cup U\}.$$

Decision making will be done on the simple classes and the classes of intersection, by neglecting the masses associated to the unions of classes which are very weak. These classes are:

$$\{U, BS, V, U \cap BS, BS \cap V, (U \cup V) \cap BS\}.$$

The result of multisource classification and fusion based on the hybrid model is given by Fig. 22.8.

The evaluation of the result obtained by multisource fusion using the hybrid model will always focus to the invariant sites between the dates 1997 and 2001. We note that the multisource image obtained by the hybrid model $M(\Theta)$ and more exactly in the airport's runways constitutes of pure classes as the class U on which the two sensors give a common opinion and the class of intersection as the class $BS \cap V$ on which the two sensors give a different opinion. This result is well illustrated by the trace of the spectral signatures (Fig. 22.9) of a pixel of airport's runways the belonging to the class of intersection $BS \cap V$.

In multitemporal fusion, we see that there is a change of themes which has occurred on the agricultural zone in the south of the airport. A great change of the Bare Soil (origin) towards Vegetation (destination). The validation of this result is

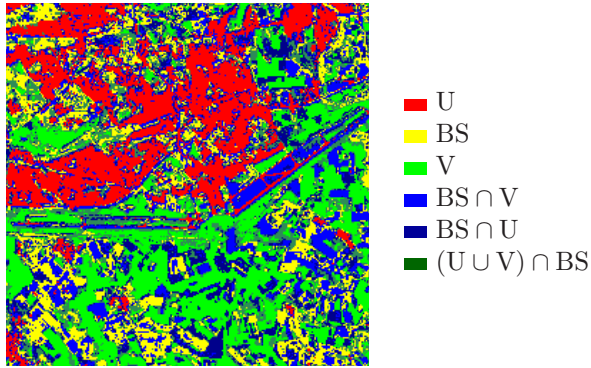


Figure 22.8: Result of multi-source fusion based on the hybrid model.

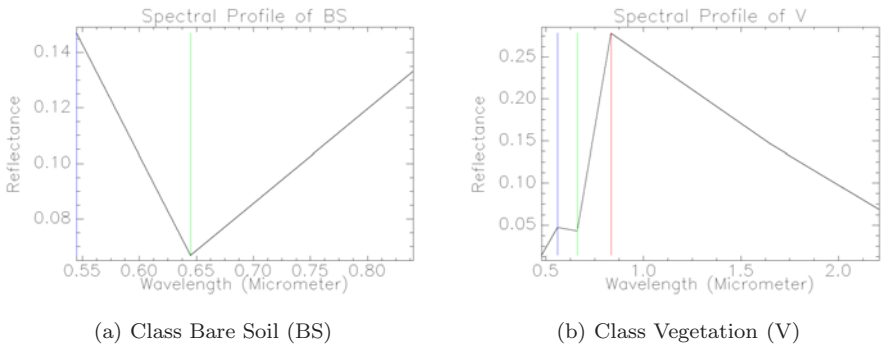


Figure 22.9: Spectral signatures of the classes bare Soil (HRV 1997) and Vegetation (ETM+ 2001) in the invariant site of the airport’s runway by the hybrid model.

done by taking a pixel belonging to the class $BS \cap V$ and then, to observe its variation between 1997 and 2001.

From the spectral signatures of Fig. 22.10, we see that a pixel of the class “Bare Soil” in this variant site in 1997 changed class after four years towards the simple class “Vegetation”.

In the multisource and multitemporal fusion using the hybrid model, the binary changes map obtained is the same one as for the free model, that is due to the decision

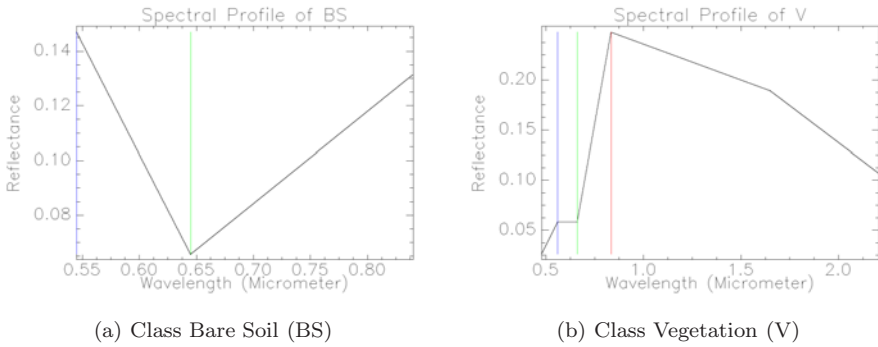


Figure 22.10: Spectral signatures of the classes Bare Soil (HRV 1997) and Vegetation (ETM+ 2001) in the variant site of the agricultural zone by the hybrid model.

rule which we applied. The pixels which represent no change (simple classes) are the pixels which belong to the same simple class in the two results obtained by Maximum Likelihood (ML). On the other hand, the pixels which represent the change are the pixels which belong to compound classes.

The only difference between both change maps is at the level of the compound classes. In case of the free model, the number of change classes is greater than the number of change classes in case of the hybrid model.

22.4.4 Comparison between the free and hybrid models

After having obtained the land cover map and changes map using the free and hybrid models of DSmT, we carried out a comparative study between these two models. The various results of this study are listed on Table 22.1.

22.5 Conclusion

Multisource classification using the free model of DSmT presents an image composed from simple classes on which both acquisition sensors (ETM + and HRV) express the same opinion, and compound classes (intersection of classes) on which the two sensors express different opinions, relatively to the multitemporal classification that provides a changes map composed of simple classes representing stable areas which have not undergone any change, and compound classes represent the change areas

	Free model	Hybrid model
Cardinality of hyper-power set	Important, according to the number of Dedekind	Reduced, according to the introduced constraints
Computing time	Important and for $n \geq 6$ very important	Acceptable
Size of memory needed	Important and for $n \geq 6$ insufficient	Sufficient
Obtained image	Includes non-significant classes	Includes more realistic classes

Table 22.1: Comparison between the free model and the hybrid model.

during the time considered. To obtain these results, we require much computing time. On the other hand, the hybrid model allows to have maps composed of classes more significant and concordant with the ground reality. The results obtained will be exploited in cartography.

We propose as possible prospects for our work: the integration within the fusion/classification process different types of satellite data known as heterogeneous for example: the contextual information or a satellite image from SAR (Synthetic Aperture Radar) to include topographic information or relief of the surface to classify for a more realistic and optimal, the use of the recent data and the update of the training base, the use of other rules of combination such as the PCR5 (Proportional Conflict Redistribution), URR (Uniform Redistribution Rule), PURR (Partially Uniform Redistribution Rule).

22.6 References

- [1] A. Appriou, *Probabilités et incertitude en fusion de données multi-senseurs*, Revue Scientifique et Technique de la Défense, Vol. 11, pp. 27–40, 1991.
- [2] I. Bloch, *Fusion d'informations en traitement du signal et des images*, IC2. Hermès Science, Paris, France, 2003.
- [3] A. Bouakache, *Fusion des images satellitaires par la théorie d'évidence et la théorie du raisonnement plausible et paradoxal*, Mémoire de magister en électronique, spécialité traitement du signal et d'images, Université des Sciences et de la Technologie Houari Boumediene, Bab Ezzouar, Alger, Algeria, 2005.
- [4] S. Corgne, L. Hubert-Moy, J. Dezert and G Mercier, *Land cover change prediction with a new theory of plausible and a paradoxical reasoning*, in [13].
- [5] A. P. Dempster, *Upper and lower probabilities induced by a multivalued mapping*, Annals of Mathematical Statistics, Vol. 38, no. 2, pp. 325–339, 1976.

- [6] J. Dezert, *An introduction to the theory of plausible and paradoxical reasoning*, in Proc. of NM&A 02, pp. 20–24, Borovetz, Bulgaria, Aug. 2002.
- [7] J. Dezert, *Fondations pour une nouvelle théorie du raisonnement plausible et paradoxal: Application à la fusion d'informations incertaines et conflictuelles*, Tech. Rep. 1/06769 DTIM, ONERA Tech. Rep., 2003.
- [8] J. Dezert, F. Smarandache, *On the generation of hyper-power sets for DS_mT*, in Proc. of Int. Information Fusion Conf., pp. 1118–1125, Cairns, Australia, 2003.
- [9] J. Dezert and F. Smarandache, *Partial ordering of hyper-power sets and matrix representation of belief functions within DS_mT*, in Proc. of Int. Information Fusion Conf., pp. 1230–1238, Cairns, Australia, 2003, .
- [10] R. Khedam, A. Bouakache, G. Mercier and A. Belhadj-Aissa, *Fusion multirate à l'aide de la théorie de Dempster-Shafer pour la détection et la cartographie des changements : application aux milieux urbain et périurbain de la région d'alger*, Télédétection, Vol. 6, no. 4, pp. 359–404, 2006.
- [11] S. Le Hégarat-Masclé, I. Bloch and D. Vidal-Madjard, *Application of Dempster-Shafer evidence theory to unsupervised classification in multisource remote sensing*, IEEE Trans. Geosci. Remote Sensing, vol. 35, no. 4, pp. 1018–1031, 1997.
- [12] S. Le Hégarat-Masclé, D. Richards and C. Ottlé, *Multi-scale data fusion using Dempster-Shafer evidence theory*, Integrated Computer-Aided Engineering, IOS press, 2003.
- [13] F. Smarandache, J. Dezert (Editors), *Advances and Applications of DS_mT for Information Fusion (Collected works)*, American Research Press, Rehoboth, U.S.A., 2004.
- [14] F. Smarandache, J. Dezert (Editors), *Advances and Applications of DS_mT for Information Fusion (Collected works)*, vol. 2, American Research Press, Rehoboth, U.S.A., 2006.
- [15] F. Smarandache, J. Dezert, *Fusing uncertain, imprecise and paradoxical information (DS_mT)*, Information & Security an international journal, Vol. 20, pp. 06–152, 2006.
- [16] G. Shafer, *A Mathematical Theory of Evidence*, Princeton University Press, Princeton (NJ), 1976.
- [17] Ph. Smets, *The combination of evidence in the transferable belief model*, IEEE Trans. Pattern Anal. Machine Intell., Vol. 12, no. 5, pp. 447–458, 1990.